Long-Term Toxicity and Uptake of Silver Nanomaterials to Relevant Plant Species

Kathleen Marsh

Jie Liu, Ph.D., Duke Department of Chemistry
Danielle Gorka, Ph.D., National Institute of Standards and Technology

Submitted to the Duke Chemistry Department in partial fulfillment of the requirements for graduation with distinction

4/23/2018

Abstract

Over the past decade, the use of silver nanomaterials has grown significantly, predominantly due to the favorable properties that they can impart upon new and existing products (e.g. effects include antimicrobial, optical, electronic). However, due to the increased use, concerns have arisen over increased silver nanomaterial presence in the environment and their potential toxicological impacts to various organisms, especially to agricultural plants. To investigate an aspect of these concerns, we performed a study to analyze the long-term impact of differently shaped silver nanomaterials on the growth of the plant species *Lolium multiflorum* (ryegrass) in a soil medium over 28 days. An uptake study was developed in collaboration with researchers at Virginia Tech using Raman-based particle tracking to determine the location of the silver material within plant roots. While short-term studies in aqueous media with these plant species in earlier literature showed significant growth inhibition of both roots and shoots, this was not observed in the long-term soil study. Like short-term studies, the shoots in soil showed greater toxicological differences and a more consistent trend of growth inhibition than roots. However, the long-term soil study also reflected that significant toxicity differences were inconsistent between roots and shoots based on both the silver nanomaterial shape and dose, showing results of both inhibited and enhanced growth. The Raman-based particle tracking was inconclusive and yielded fluorescent bands with weak intensity of the silver materials, so localization within the roots could not be accurately determined. While shape-dependence of silver nanomaterials still requires significant research in both short- and long-term studies of various plants, this research shows silver nanomaterials interact differently in a soil medium compared to an aqueous medium.

Introduction

I. Applications of Nanomaterials

Nanomaterials (NMs) are being increasingly used in the world today for various industrial and commercial applications. NMs have useful optical, electrical, and thermal properties that are being used in photovoltaic devices, molecular diagnostics, antimicrobial coatings, and biological sensors.[1,2,3,4] Of these, silver nanomaterials (AgNMs) are among the most commonly produced due to their antimicrobial properties, as well as their facile synthesis.[3,5] AgNMs can be found in wound dressings, athletic clothing, food storage devices, and many other consumer products.[1,2,3] Silver nanoparticles (AgNPs) can be synthesized rapidly and simply, and thus are well-studied materials, but other shapes of AgNMs are being increasingly made for commercial use, such as silver nanowires (AgNWs) and silver nanocubes (AgNCs).[2]

II. Entrance into the Environment

AgNMs are released from consumer goods and other products when exposed to water. The majority are transported to wastewater treatment plants, incorporated into sewage sludge, and are eventually applied to agricultural fields.[3,4,6] Since AgNMs are being increasingly used for their antimicrobial properties in consumer products, their presence in agricultural fields is expected to increase, and thus have an increased chance of affecting soil and plants. The toxic effects of these AgNMs are still not well-known, nor are their long-term implications for environmental and human health.

III. Toxicity to Plants

Studies regarding AgNMs and their phytotoxicity include uptake of AgNPs into various species (e.g. rice, soybeans, alfalfa, and *Arabidopsis thaliana*) to analyze transport mechanisms.[7,8] These have shown that AgNMs reduce plant growth and can have an impact on food chains. Different plant species have exhibited different toxic effects from AgNMs. Phytotoxicity to *Arabidopsis thaliana* cannot fully be explained by the presence of Ag^+, while Ag^+ is important to AgNP toxicity of algae.[9,10,11,12] Various toxicity factors of AgNMs are still being studied: such as dissolution, sulfidation, and the unique toxicity specific to AgNMs.[5,12,13,14] The results have shown that dissolution of AgNPs to Ag^+ are toxic to the plant, but the AgNPs themselves may exhibit their own toxicity.[8,12] A significant metric in toxicity determination is the surface area-to-volume (SA:V) ratio of AgNMs. However, the toxicity of AgNMs cannot fully be explained by this ratio.[15] Other factors, such as shape-dependence, must be investigated to further understand the unique toxicity properties of AgNMs.

IV. Long-Term Impact, Shape-Dependence of Toxicity and Uptake

Studies of AgNM toxicity are relatively new and there is still ambiguity regarding their uptake in various plants, as well as different shapes of AgNMs. Most of the previous research on AgNMs has shown that the uptake and transport of AgNPs varies from plant to plant, with their mechanisms still unknown.[7,8,16] Additionally, little has been done to study the uptake and toxicity of other AgNM shapes, such as cubes and wires. Previous experiments have mainly investigated long-term toxicity and bioavailability of AgNPs and short-term toxicity comparing different shapes of AgNMs to one another.[3,12,15,17] Raman spectroscopy, specifically Surface Enhanced Raman Spectroscopy (SERS), has frequently been employed for uptake studies due to

the presence of fluorescent silver bands.[13,18,19] Since the majority of previous uptake studies have shown that silver transport varies among plant species, the fate of location of these AgNMs after uptake is unclear, but they appear to accumulate in the root tips of *Arabidopsis thaliana*.[18,19,20] Additionally, Stegemeier, et. al. showed that AgNPs accumulated in the elongation zone of alfalfa plants.[17] However, little work has been done to examine the uptake of AgNMs with different shapes. By investigating shape-dependent effects and uptake mechanisms of these AgNMs over a long-term study, a better understanding of their trophic movement and unique phytotoxicity will be uncovered.

This project examined the shape- and dose-dependence of AgNM phytotoxicity and uptake to a model plant species through long-term studies in a synthetic soil medium. Specifically, three AgNMs: AgNPs, AgNCs, and AgNWs were studies in the ryegrass *Lolium multiflorum*. Additionally, uptake studies were conducted using surface enhanced Raman spectroscopy (SERS) to determine the location of the AgNMs in plant roots. Studying long-term toxicity and uptake of these AgNMs provided knowledge about how nanomaterial shape can affect plants in more realistic and environmentally relevant scenarios

Methodology

I. AgNM Synthesis

The AgNMs were synthesized via commonly utilized polyol protocols, and were coated with polyvinylpyrrolidone (PVP, MW 55 kDa, Aldrich).[3,5] All AgNMs were stored in the dark until use. The AgNPs were synthesized as follows: First, 2 g of PVP was dissolved into 5 mL anhydrous ethylene glycol (Ampresco) while stirring at room temperature. Next, 150 mg of silver nitrate ($AgNO_3$, 99.999%, Alfa Aesar) was dissolved into the solution while stirring. The solution was

then heated to 145 °C to react for 24 h. Afterwards, the AgNPs were purified by rinsing with acetone and centrifuged at 7000 rpm for 1 h. Finally, the AgNPs were resuspended in 10 mL of PicoPure water (18 MΩ, Hydro Picopure UV Plus, Durham, NC, USA).

AgNC synthesis is as follows: 6 mL of anhydrous ethylene glycol was heated at 154 °C for 1 h while stirring. Next, 5 μL of sodium hydroxide (NaOH, 200 mM in ethylene glycol, 98.6%, Fisher), 80 μL sodium sulfide nonahydrate (3 mM in ethylene glycol, 99.999% Aldrich), 1.5 mL PVP (20 mg/mL in ethylene glycol) and 24 mg $AgNO_3$ (0.5 mL, 48 mg/mL in ethylene glycol) were quickly and sequentially added to the ethylene glycol. The solution was heated for 8 min, as the solution changed color—starting from a clear yellow and finishing with an opaque ruddy brown. The solution was taken off the heat, cooled to room temperature, and rinsed in acetone. This suspension was centrifuged at 7000 rpm for 9 min, and then the AgNCs were resuspended in 5 mL PicoPure water.

The AgNWs were synthesized as follows: 5 mL of anhydrous ethylene glycol was heated in a round bottom flask for 10 min at 160 °C under bubbling nitrogen. After 10 min, the nitrogen was removed and the solution was heated with stirring for another 50 min. 48 mg PVP (144 mM in ethylene glycol), sodium chloride (220 μM in ethylene glycol, Fisher), and iron nitrate (iron nitrate nonahydrate, 22 μM in ethylene glycol, Aldrich) were prepared in a 3 mL solution with an ethylene glycol solvent. Additionally, a 3 mL solution with 48 mg $AgNO_3$ (94 mM in ethylene glycol) was prepared in anhydrous ethylene glycol. Both of these solutions were simultaneously injected into the round bottom flask using a syringe pump (New Era Pump Systems Inc., Farmingdale, NY, USA) at a rate of 45 mL/h. The solution continued to be heated with stirring for 1 h. During this reaction, the solution transitioned from colorless to an opaque

tan color. After 1 h, the solution was cooled to room temperature, rinsed in acetone, centrifuged at 4500 rpm for 10 min, and the AgNWs were resuspended in 10 mL PicoPure water.

II. AgNM Characterization

All AgNMs were characterized using a Tecnai G^2 Twin transmission electron microscope (TEM, FEI, Hillsboro, OR, USA) at 160 kV and an FEI XL30 SEM-FEG scanning electron microscope (SEM, FEI, Hillsboro, OR, USA) to collect images to determine the size of the AgNMs. Their lengths were measured using ImageJ (National Institutes of Health, Bethesda, MD, USA). For size the diameter of AgNPs, edge length of AgNCs, and diameter and length of AgNWs are reported. Size is reported as mean $\pm$ standard error. Surface area was determined assuming the AgNMs were perfect spheres, cubes, and pentagonal prisms, respectively. It was imperative to ensure that the AgNMs were not aggregated—AgNM toxicity can be altered, and toxicity analysis can be inaccurate, due to smaller surface area of the materials in aggregated nanomaterials. UV-Vis spectroscopy was utilized to further characterize the AgNMs using a Varian Cary 60 Conc spectrophotometer (UV-Vis, Agilent, Santa Clara, USA). A PerkinElmer atomic absorption spectrophotometer (PerkinElmer, 3100, Waltham, MA, USA) was employed to determine the concentration of the suspended AgNMs. The AgNM concentrations were calculated using a calibration curve given in Appendix A (Figure A1).

III. Long-Term Soil Procedure

Synthetic soil was made for this experiment following the Organisation for Economic Co-operation and Development (OECD) guidelines: 70% quarts silica sand (Quikrete, Atlanta, GA, USA), 20% EPK Kaolin clay (Edgar Minerals, Hawthorne, FL, U.S.A.), and 10% sphagnum peat

moss (Scott's Miracle-Gro Co., Marysville, OH, USA) .[21,22] Four hundred grams of homogenous soil was added to each 4"x4" pot, with 9 seeds of *L. multiflorum*, as shown in Figure 4. An initial 50 mL dose of PicoPure water, AgNP, AgNW, or AgNC solution at concentrations of 1 ppm, 5 ppm, 10 ppm, 50 ppm, or 100 ppm were added to each pot. For the following 29 days, each pot was watered daily with between 10 mL and 30 mL of PicoPure water to maintain saturated soil. Temperature and humidity were monitored three times per day to ensure a consistent growth environment. After 27 d, roots and shoots were extracted from soil, separated from one another, and length was measured individually.

IV. Analysis of Phytotoxicity

Root and shoot length for the unique AgNM shapes and doses were measured using digital calipers to discover potential differences. Statistical analysis of the root and shoot length of the long-term study was carried out using 2-way factorial Analysis of Variance (ANOVA) in JMP 13 Pro Software (SAS Institute Inc., Cary, NC, U.S.A). Tukey-Kramer analysis was conducted to determine differences between doses of AgNMs in *L. multiflorum* roots and shoots. Statistically significant differences in Tukey-Kramer analysis, where $p<0.05$, were indicated with a letter change: A, B, C. A combination of letters, such as AB, indicated differences significant at $p<0.1$. Values are plotted as mean $\pm$ standard error. The data excluded plants that did not germinate.

V. Raman-Based Particle Tracking

A collaboration was conducted with Dr. Peter Vikesland and Dr. Weinan Leng of Virginia Tech using SERS to visualize the uptake using *L. sativa* roots. The measurements were performed with a WITec alpha 500 confocal Raman system equipped with a 100x Olympus

objective (Instrument Corp., Knoxville, TN, U.S.A.). A 785 nm diode laser and 300 grooves/mm grating were used to collect Raman scatterings. In order to find the silver associated Raman signals, a stack image scan from top of the root to bottom was performed for each sample. A 0.1 s integration time was applied for each spectrum collection. To localize Ag particles, the integrated intensity of band wavenumber ~250 cm^{-1} for Ag-O was set to produce particle 2-dimensional images. The fluorescent intensity between 1450-1550 cm^{-1} from the root was used to generate plant structure.

Results and Discussion

Figure 1 shows the TEM results of AgNM characterization. Figures 1A, 1B, and 1C show images of AgNPs, AgNCs, and AgNWs, respectively. Measurements of images similar to Figure 1 were used to further characterize the size of the AgNMs shown in Table 1. AgNM mean size $\pm$ standard error were determined, and used to calculate solution concentrations and the surface area of each AgNM. AgNPs (41.3 nm diameter) and AgNCs (38.4 nm edge length) were much smaller in size than the AgNWs (77.5 nm width, 4.6 μm length). Thus, their surface areas were comparable to one another, and slightly more than double that of the AgNWs. However, the particle concentration of AgNPs and AgNCs was larger than AgNWs by approximately 3 orders of magnitude.

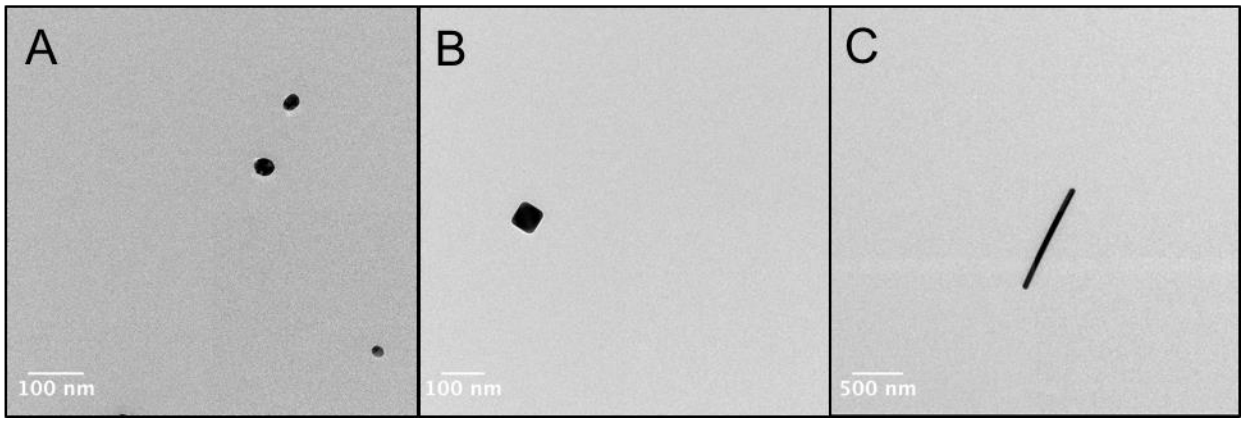

Figure 1. Transmission electron microscopy images of silver nanomaterials. A) silver nanoparticles; B) silver nanocubes; C) silver nanowires.

Table 1. Mean and standard error of size, concentration, and surface area of AgNMs at 10 ppm Ag. Sizes are defined as diameter (AgNP), edge length (AgNC), and length and width (AgNW).

Sample	**Size (nm)**	**Concentration (particles/mL)**	**Surface Area (cm^2/mL)**
AgNP	41.3 ± 12.0	$2.85x10^{12} \pm 1.33x10^{12}$	152.5 ± 118.2
AgNC	38.4 ± 5.5	$1.85x10^{12} \pm 1.24x10^{12}$	164.1 ± 143.5
AgNW	L: 4649.5 ± 2571.6 W: 77.5 ± 21.9	$5.18x10^{9} \pm 2.03x10^{9}$	61.0 ± 47.5

Toxicity was defined as a significant decrease in root or shoot growth. Growth was compared between different shapes and doses using *L. multiflorum*. Data using AgNPs for *L. sativa* and *S. lycopersicum* is shown in Appendix A. A significant difference in root or shoot length was defined as having a p-value of $p<0.05$. A dose of 0 ppm in the following figures indicated the control measurements, where no AgNMs were dosed to the plants, only PicoPure water.

The progression of the plant growth of *L. multiflorum* throughout the long-term experiment, which lasted 28 d, is shown in Figure 2. The most rapid plant growth—for all doses and shapes—was observed in the first week, and was much slower for the remainder of the experiment.

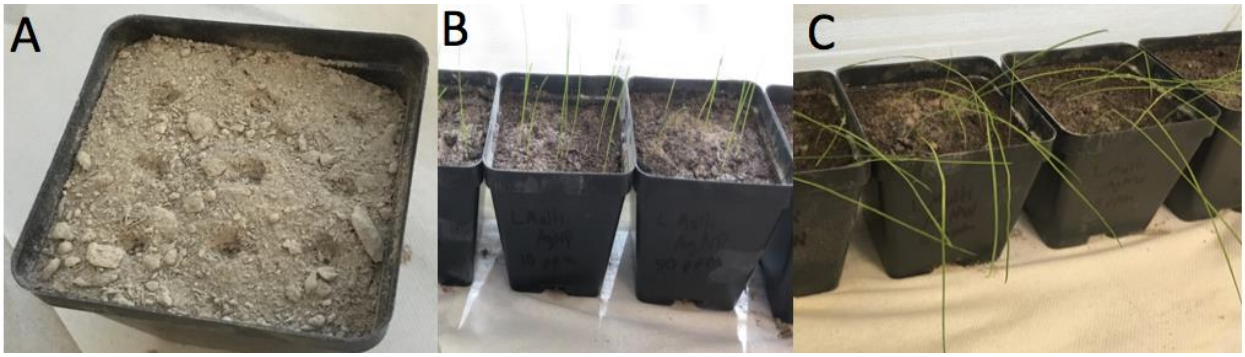

Figure 2. *L. multiflorum* growth progression from left to right: A) Day 0; B) Day 7; C)Day 21

Table 2 displays the 2-way factorial ANOVA analysis for shape- and dose-dependent toxicity of *L. multiflorum* roots and shoots. The columns *Prob>F* for roots and shoots indicate the significance of difference of both individual variables, both shape and dose, as well as the effect of dose and shape combined. Values with an adjacent star indicate significant differences in root or shoot length at $p<0.05$. Thus, only dose caused significant toxicity in roots, but shape, dose, and both shape and dose combined caused significant toxicity in shoots.

Table 2. Two-Way Factorial ANOVA of shape and concentration of shape and concentration effects on *L. multiflorum* roots and shoots. * indicates significant differences at $p<0.05$.

Variable	Prob>F (roots)	Prob > F (shoots)
Shape	0.8691	<0.0001*
Dose	0.0018*	<0.0001*
Shape*Dose	0.1538	<0.0001*

I. Roots

As shown in Table 2, the only significant variable impacting toxicity in the roots of *L. multiflorum* was dose, where increasing dose resulted in decreasing root growth. Figures 3 and 4 shows the least squares means plots of *L. multiflorum* roots based on different shapes and doses of AgNMs, respectively. Analysis of shape alone did not cause significant differences in toxicity. Figure 3 showed little variation between mean root lengths of AgNCs, AgNPs, and AgNWs, which 2-way ANOVA determined was not significant. Figure 4 showed a small but

significant downward trend in root length Ag doses at or above 1 ppm. While toxicity trends were visualized in both these figures, data showed significant differences were only found for dose, where increasing dose resulted in decreased root growth.

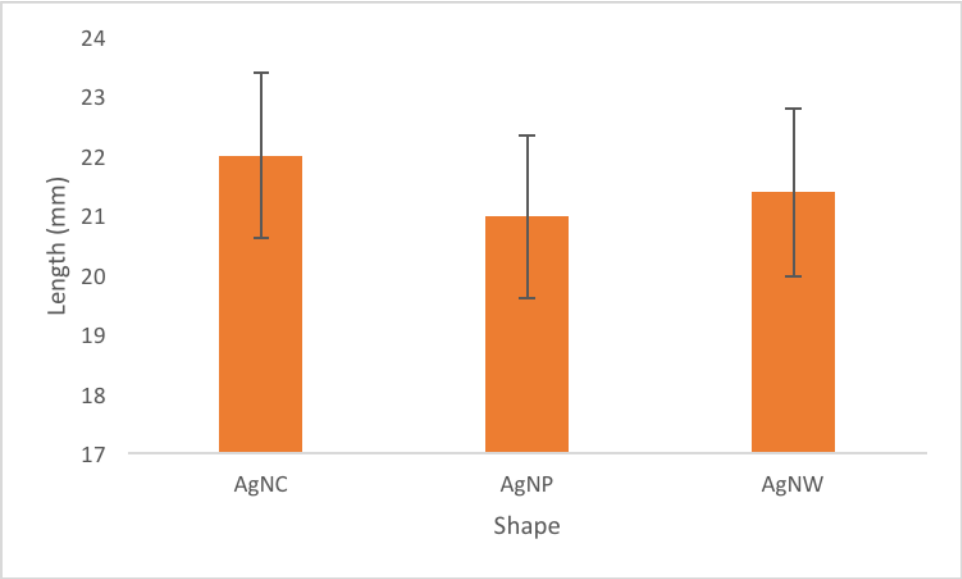

Figure 3. Least square means plot of *L. multiflorum* roots based on exposure to different shapes of silver nanomaterials. The error bars indicate standard error of mean root length.

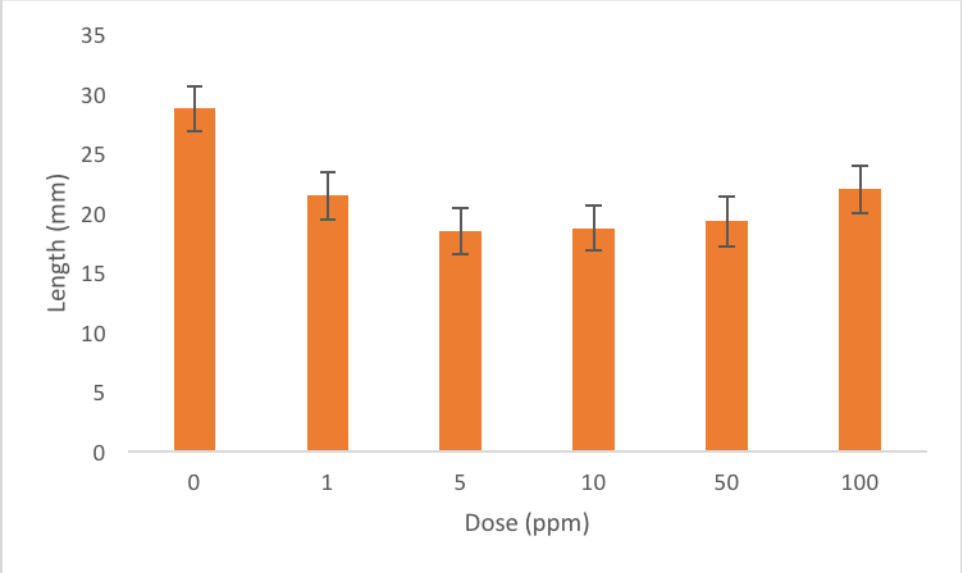

Figure 4. Least square means plot of *L. multiflorum* roots based on different doses of silver nanomaterials. The error bars indicate standard error of mean root length.

The root lengths of *L. multiflorum* roots based upon both dose and shape were plotted in Figure 5. When accounting for both shape and dose combined, no significant decrease in root length was observed. Mean root length is approximately equal among the 3 shapes at doses of 1 ppm, 5 ppm, and 10 ppm. However, at doses of 50 ppm and 100 ppm, different shapes of AgNMs show different toxicity. No particular shape consistently showed more or less toxicity. There was minimal variation in root length among all three AgNM shapes with increasing doses. However, the combination of both shape and dose did not result in significant toxicity and instead showed inconsistent differences. While roots only showed dose-dependent toxicity, analysis of shoots was also performed to determine if shoots showed toxic effects not found in roots.

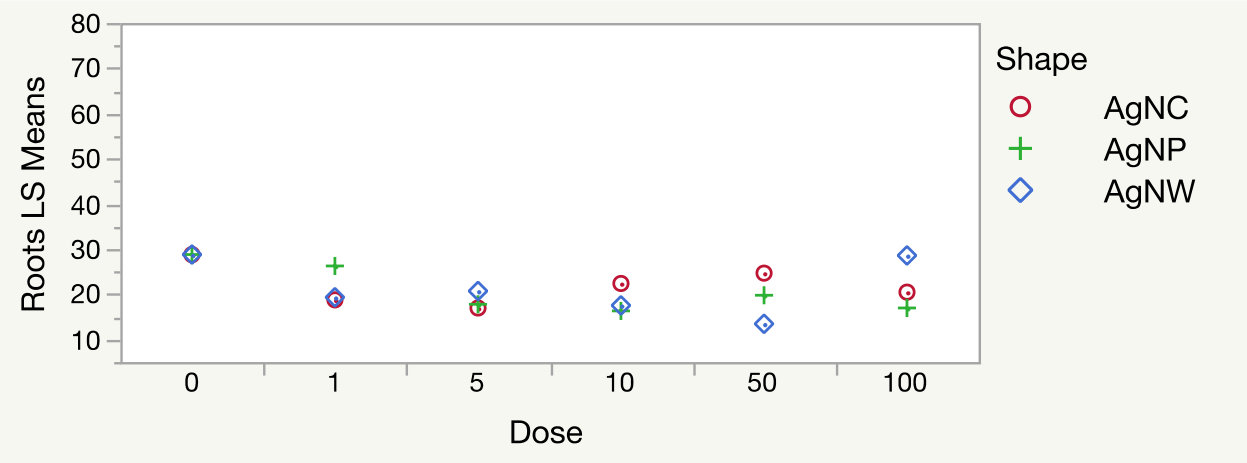

Figure 5. The toxic effects of both silver nanomaterial shape and dose on *L. multiflroum* roots.

II. Shoots

Toxicity differences in both shape and dose were visualized in Figures 6, 7, and 8, and 2 way ANOVA (Table 2) confirmed that these variables caused significant differences in shoot growth. Figures 6 and 7 are the least squares means plots of *L. multiflorum* shoots based on shape and dose of AgNMs, respectively. Figure 6 displays differences in shoot length among

AgNPs, AgNCs, and AgNWs. The AgNCs had the shortest mean shoot length, which indicated they were more toxic than AgNPs and AgNWs. However, there was little variation in mean shoot length between AgNPs and AgNWs, suggesting the two shapes had similar toxicity. Figure 7 showed a decrease in mean shoot length with increasing dose. Increasing dose resulted in deceased growth across the doses tested, except plants exposed to 10 ppm AgNM had more growth than those exposed to 5 ppm AgNM. However, the decreased growth was significant and more visibly apparent in roots.

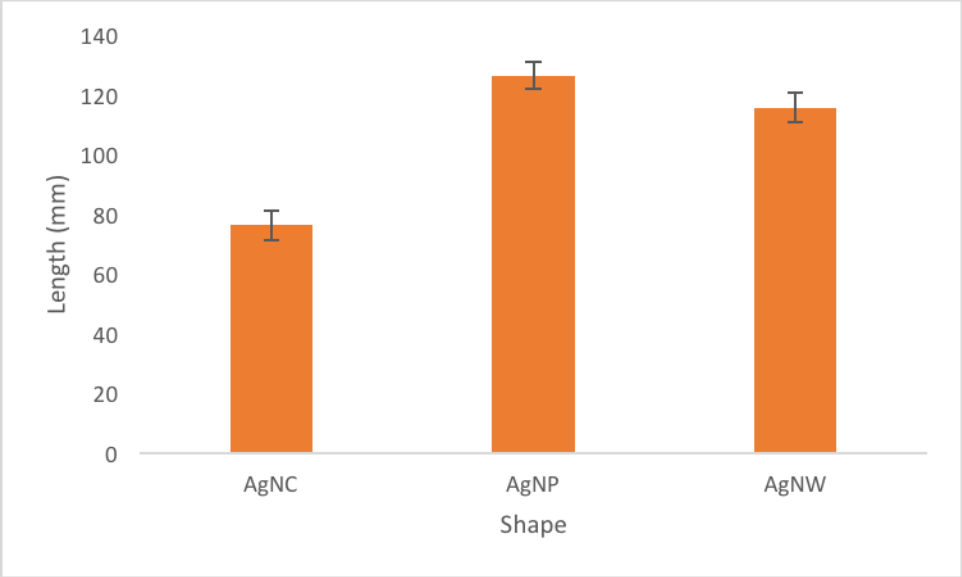

Figure 6. Least square means plot of *L. multiflorum* shoots based on exposure to different shapes of silver nanomaterials. The error bars indicate standard error of mean root length.

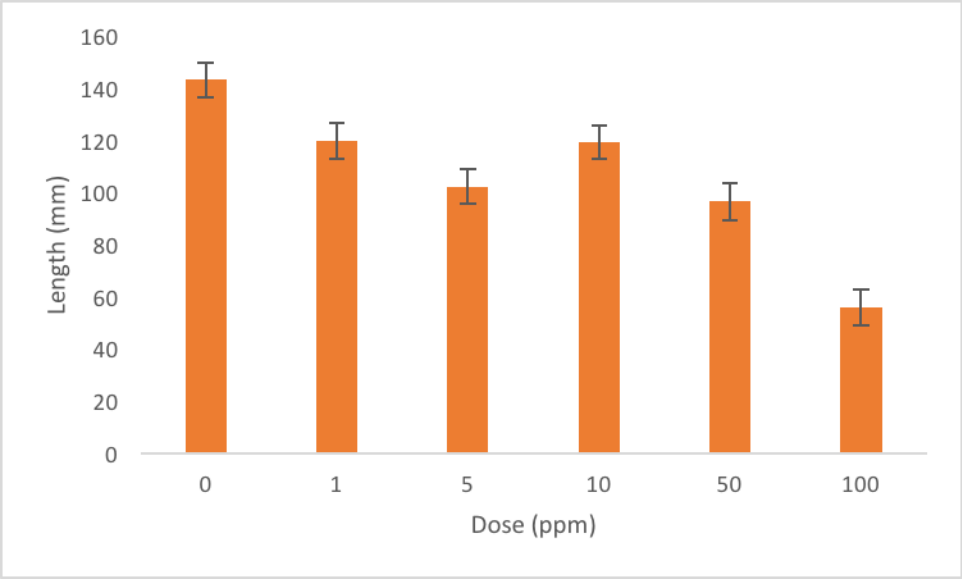

Figure 7. Least squares means plot of *L. multiflorum* shoots based on different doses of silver nanomaterials. The error bars indicate standard error of shoot length.

The mean lengths of *L. multiflorum* shoots based upon both dose and shape combined were plotted in Figure 8. As shown in Table 2, both shape and dose combined were found to cause significant toxicity to shoots. Shoot lengths showed greater response to AgNMs than roots. Nearly all shapes at higher doses showed greater toxic effects than the control, with the exception being AgNP shoots at 1 ppm and 10 ppm. These instances of growth enhancement in shoots were consistent with the hormetic effect found in other AgNM toxicity studies, where subtoxic metal exposure was beneficial to plant growth. [23,24] Generally, AgNPs and AgNWs showed similar decreased growth with increasing dose. However, AgNCs behaved differently, and showed a much larger initial decrease in growth than the other AgNMs, though it remained consistent across doses until 100 ppm, where all shapes had comparable lengths.

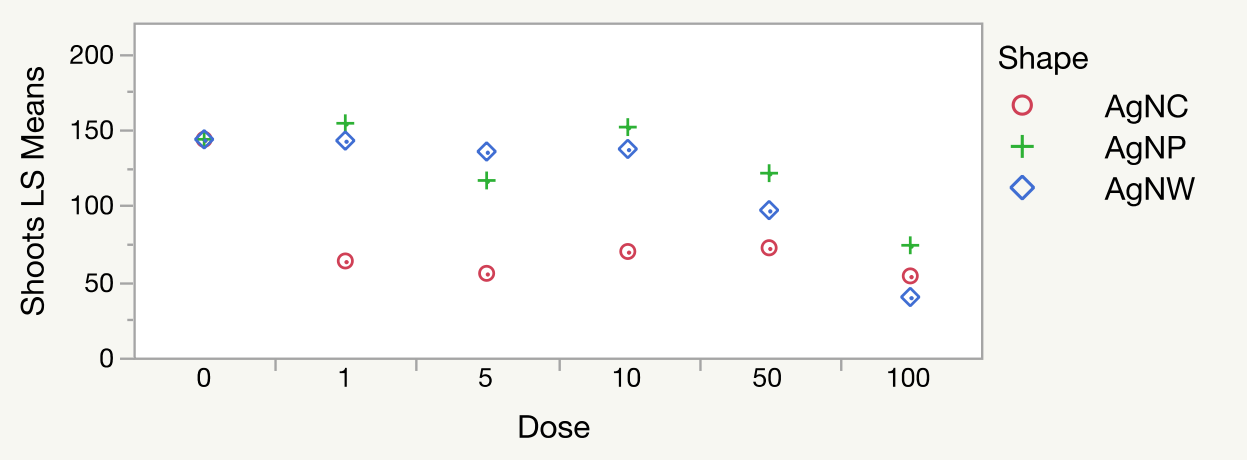

Figure 8. The toxic effects of both silver nanomaterial shape and dose on *L. multiflorum* shoots.

After examining AgNM toxicity, it was apparent that shoot growth was impacted more than root growth. While dose was significant in both roots and shoots, shape was a significant predictor of toxicity only in the shoots. These toxicological differences in AgNM shapes can be partially attributed to a variety of factors: such as uptake, dissolution, soil affinity, and AgNM aggregation. [8,10,13,17] Prior literature has shown that plant uptake is greater in smaller-sized AgNMs, such as the AgNPs and AgNCs compared to the AgNWs. Additionally, aggregated materials exhibit different toxicological properties than AgNMs, and any AgNMs that may have become aggregated upon addition to soil may result in less uptake and toxicity. Increased dissolution of AgNMs may also create toxicity differences, and thus should undergo more study.

III. Uptake

To better understand the toxic effects of AgNMs in plants, their uptake was examined using SERS. SERS was used because of its ability to enhance Raman scattering and detect single molecules. In this experiment, this technique was aimed at determining the location of PVP-coated AgNMs within the plants. *L. sativa,* lettuce, was examined due to its rapid germination and growth. The background fluorescence was colored green, while the AgNM fluorescence

was colored teal in the cross sectional images (Figure 9). Higher CCD counts indicated a higher concentration of electrons fluorescing at a particular location. The fluorescence from plant electron scattering was much stronger than the scattering from the AgNMs due to the natural fluorescence of the plant. Observing AgNM location was difficult due to the weak fluorescence.

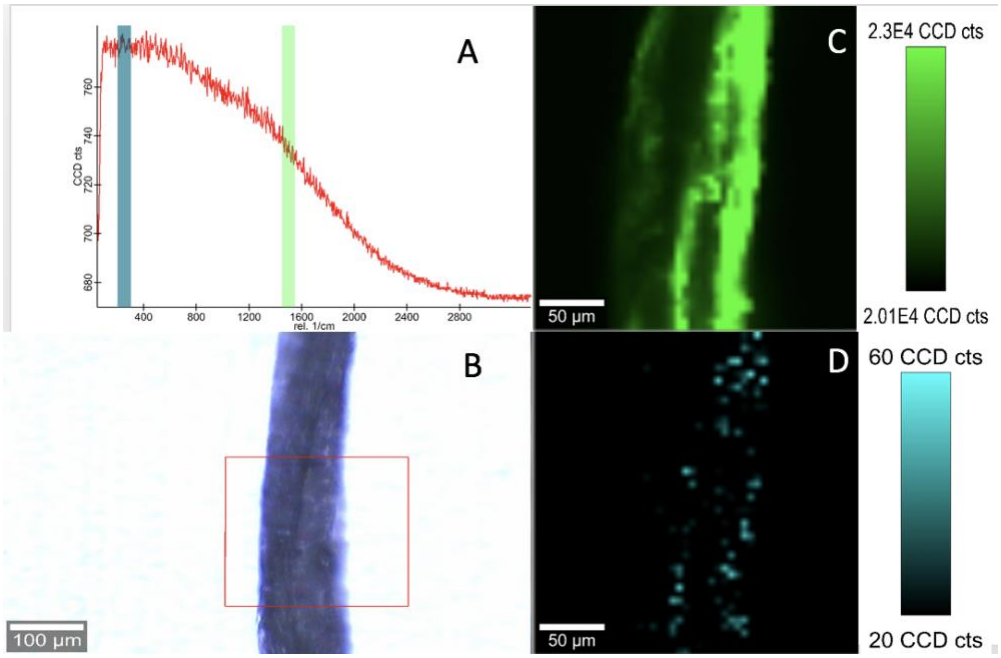

Figure 9. *L. sativa* roots dosed with 10 ppm AgNWs. A) A typical Raman spectrum (including fluorescent background); B) Cross sectional image location; C) Fluorescent background in the root; and D) Fluorescent spectra at the Ag fluorescent peak indicating the AgNW locations in the root.

The results of the uptake study using SERS were not robust enough to make definitive conclusions, however some useful information was gained. The AgNWs appear to localize on the edges of the root, with almost no AgNM fluorescence intensity in the center of the cross-sectional areas of the roots (Figure 9). While Figure 9 only shows AgNW fluorescence in *L. sativa* roots, both AgNPs and AgNCs could also be observed in exposed *L. sativa* roots, and displayed similar results. This work follows similar results to Quah, et. al., and Ma, et. al., which found that AgNPs were localized in the edges and tips of the roots of *Triticum aestivum* (wheat) and

Crambe abyssinica (oilseed), respectively.[13,25] Similarly, Stegemeier, et. al. showed AgNPs localized in elongation zones of plants, while Ag^+ showed consistent distribution throughout the roots.[17] AgNMs show unique uptake compared to ionic silver, indicating differences in plant affinity and transport. Raman-based particle tracking needs a reliable Raman band associated with the particles themselves. For PVP coated AgNMs, the most enhanced Raman signal is the Ag-O coordination bond at the vibrational frequency of ~240-250 cm^{-1}. In the results from this study (Figure 9), the band was too weak to be sufficiently differentiated from the background, due to the heavy PVP coating on the AgNWs. While Figure 9D shows some localization on the root tips and edges, a stronger band must be acquired in Raman-based particle tracking to make more definitive statements. In order to more accurately determine the location of AgNMs within the roots, a more effective particle tracking technique must be used, or should be used in conjunction with this technique. This experiment only investigated roots, while shoots were not analyzed. Further investigation of AgNM uptake needs to be conducted, including examination of shoots, before definitive conclusions about AgNM uptake can be made.

Conclusions and Future Work

L. multiflorum root growth showed dose-dependent effects and shoot growth showed both shape- and dose-dependent effects after AgNM exposure. It is important to note that the plant shoot growth had more significant differences in length than roots, making them more useful in analyzing shape-based AgNM toxicity. In *L. multiflorum* roots, the only significant indicator of toxicity was dose. Shape did not show a significant effect on root growth. A significant decrease in root length of all doses compared with the control was observed ($p<0.0018$). Significant toxicity also was also shown in *L. multiflorum* shoots based upon shape,

dose, and both variables combined ($p<0.0001$). The plants dosed with AgNCs exhibited significantly greater toxic effects than those exposed to AgNPs and AgNWs. The effect of dose on shoots was similar to the roots, with significant decreases in growth as dose increased. The combination of both shape and dose was also significant: AgNCs experienced the greatest decreases in shoot length, and increasing dose generally decreased the shoot length. However, some enhancement of growth was observed at doses of 1 ppm and 10 ppm AgNPs, consistent with the hormetic effect. While shape and dose have been shown to predict toxicity, a variety of other factors also affect their toxicity, and must be studied further.

Further investigation of this work should include more frequent dosing of AgNMs into the soil, as well as long-term studies over a duration greater than 28 days. Dosing the plants with AgNM solution on a daily basis, representing a more realistic exposure scenario, may yield trends similar to the short-term studies showing increased phytotoxicity. Performing an experiment allowing plants to grow to maturity is also important for future study to more closely resemble agricultural conditions. Additionally, a more successful uptake study requires a stronger Raman signal in PVP-coated AgNMs, or a more effective particle-based tracking method for these materials should be utilized. While SERS was only conducted in roots for this experiment, both roots and shoots should be examined in future work, with multiple cross-sectional images taken in order to visualize the entire plant in order to more effectively determine localization and uptake of these AgNMs. Long-term studies are important to further understand the impact of AgNMs on the environment, especially on products of agriculture. These results conclude that dose-dependence continues through long-term growth, and that shape also presents unique toxicity of various AgNMs. However, inconsistent growth results

showed that shape and dose are not the only predictors of long-term toxicity, and that interactions between AgNMs and soil present another factor that must be considered.

Acknowledgements

I would like to thank Jie Liu, Ph.D. and Danielle Gorka, Ph.D. for guiding this research. Additionally, I recognize invaluable contributions from Peter Vikesland, Ph.D., and Weinan Leng, Ph.D. from Virginia Tech on collaboration with Raman spectroscopy component of this project. Additionally, thank you to Dr. Roy, Dr. Baldwin, and Dr. MacPhail for teaching me techniques of scientific writing and presentation. Finally, I would like to thank the Duke Research Scholars Program for providing me with my first research opportunity in the Liu lab. This research was funded by the Duke Undergraduate Research Support office, the Duke SMIF Undergraduate User Program. This material is based upon work supported by the National Science Foundation (NSF) and the Environmental Protection Agency (EPA) under NSF Cooperative Agreement EF-0830093 and DBI-1266252, Center for the Environmental Implications of NanoTechnology (CEINT). Any opinions, findings, conclusions, or suggestions expressed in this material are those of the author(s) and do not necessarily reflect the views of the NSF or the EPA. This work has not been subjected to EPA review and no official endorsement should be inferred.

References

1. Oldenburg, Steven. Silver Nanoparticles: Properties and Applications. *Sigma-Aldrich* **2010**.
2. Lines, M.G. Nanomaterials for Practical Functinoal Uses. *Journal of Alloys and Compounds* **2008**, *449* (1–2), 242–245.
3. Gorka, Danielle E.; Osterberg, Joshua S.; Gwin, Carley A.; Colman, Benjamin P.; Meyer, Joel N.; Bernhardt, Emily S.; Gunsch, Claudia, K.; DiGuilo, Richard T.; Liu, Jie. Reducing Environmental Toxicity of Silver Nanoparticles through Shape Control. *Environ. Sci. Technol* **2015**, *49* (16), 10093–10098.
4. Benn, T; Cavanagh, B; Hristovski, K; Posner, J.D; Westerhoff, P. The Release of Nanosilver from Consumer Products Used in the Home. *J. Environ. Qual* **2010**, *39* (6), 1875–1882.
5. Wiley, Benjamin; Sun, Yugang; Xia, Younan. Polyol Synthesis of Silver Nanostructures: Control of Product Morphology with Fe(II) or Fe(III) Species. *Langmuir* **2005**, *21* (18), 8077–8080.
6. Blaser, S.A; Scheringer, M; Macleod, M; Hungerbuhler, K. Estimatino of Cumulative Aquatic Exposure and Risk Due to Silver: Contribution of Nano-Functionalized Plastics and Textiles. *Sci. Total Environ.* **2008**, *390* (2–3), 396–409.
7. Schwab, F; Zhai, G; Kern, M; Turner, A; Schnoor, J.L; Wiesner, M.R. Barriers, Pathways and Processes for Uptake, Translocation and Accumulation of Nanomaterials in Plants—Critical Review. *Nanotoxicology* **2016**, *10* (3), 257–278.
8. Geisler-Lee, Jane; Wang, Qiang; Yao, Y; Zhang, W; Geisler, Matt; Li, K; Huang, Y; Chen, Y; Kolmakov, A; Ma, Xingmao. Phytotoxicity, Accumulation and Transport of Silver Nanoparticles by Arabidopsis Thaliana. *Nanotoxicology* **2013**, *7* (3), 323–337.
9. Krishnaraj, C; Jagan, E.G; Ramachandran, R; Abirami, S.M; Mohan, N; Kalaichelvan, P.T. Effect of Biologically Synthesized Silver Nanoparticles on Bacopa Monniera (Linn.) Wettst. Plant Growth Metabolism. *Process Biochemistry* **2012**, *47* (4), 651–658.
10. Colman, Benjamin P.; Espinasse, Benjamin; Richardson, Curtis J.; Matson, Cole W.; Lowry, Gregory V.; Hunt, Dana E.; Wiesner, Mark R.; Bernhardt, Emily S. Emerging Contaminant or an Old Toxin in Disguise? Silver Nanoparticle Impacts on Ecosystems. *Environ. Sci. Technol* **2014**, *48* (9), 5229–5236.
11. Colman, Benjamin P.; Wang, S.Y.; Auffan, M.; Wiesner, M.R.; Bernhardt, Emily S. Antimicrobial Effects of Commercial Silver Nanoparticles Are Attentuated in Natural Streamwater and Sediment. *Ecotoxicology* **2012**, *21* (7), 1867–1877.
12. Yin, L; Colman, Benjamin P.; McGill, B.M.; Wright, J.P.; Bernhardt, Emily S. Effects of Silver Nanoparticle Exposure on Germination and Early Growth of Eleven Wetland Plants. *PLOS One* **2012**, *7* (10), e47674.
13. Quah, Bryan; Musante, Craig; White, Jason C.; Ma, Xingmao. Phytotoxicity, Uptake, and Accumulation of Silver with Different Particle Sizes and Chemical Forms. *Journal of Nanoparticle Research* **2015**, *17* (299), 277.
14. Nowack, Bernd; Bucheli, Thomas D. Occurrence, Behavior, and Effects of Nanoparticles in the Environment. *Environmental Pollution* **2007**, *150* (1), 5–22.

15. Gorka, Danielle E.; Liu, JIe. Effect of Direct Contact on the Phytotoxicity of Silver Nanomaterials. *Environ. Sci. Technol* **2016**, *50* (19), 10370–10376.
16. Marchiol, L; Mattiello, A; Poscic, F; Giordano, C; Musetti, R. In Vivo Synthesis of Nanomaterials in Plants: Location of Silver Nanoparticles and Plant Metabolism. *Nanoscale Res Lett* **2014**, *2* (9), 101.
17. Stegemeier, John P; Schwab, Fabienne; Colman, Benjamin P; Webb, Samuel M; Newville, Matthew; Lanzirotti, Antonio; Winkler, Christopher; Wiesner, Mark R; Lowry, Gregory V. Speciation Matters: Bioavailability of Silver and Silver Sulfide Nanopartiles to Alfalfa (Medicago Sativa). *Environ. Sci. Technol* **2015**, *49* (14), 8451–8460.
18. Lin, Sijie; Reppert, Jason; Hu, Qian; Judson, JoAn S; Reid, Michelle L; Ratnikova, Tatsiana A; Rao, Apparao M; Luo, Hong; Ke, Pu Chun. Uptake, Translocation, and Transmission of Carbon Nanomaterials in Rice Plants. *Small* **2009**, *5* (10), 1128–1132.
19. Schrader, B; Schulz, H; Andreev, G.N; Klump, H.H; Sawatzki, J. Non-Destructive NIR-FT-Raman Spectroscopy of Plant and Animal Tissues, of Food and Works of Art. *Talanta* **2000**, *53* (1), 35–45.
20. Geisler-Lee, Jane; Brooks, Marjorie; Gerfen, Jacob R; Wang, Qiang; Fotis, Christin; Sparer, Anthony; Ma, Xingmao; Berg, R. Howard; Geisler, Matt. Reproductive Toxicity and Life History Study of Silver Nanoparticle Effect, Uptake, and Transport in Arabidopsis Thaliana. *Nanomaterials* **2014**, *4* (2), 301–318.
21. Mangala, P; De Silva, C.S; van Gestel, Conelis A.M. Development of an Alternative Artificial Soil for Earthworm Toxicity Testing in Tropical Countries. *Applied Soil Ecology* **2009**, *43*, 170–174.
22. Shoults-Wilson, W. Aaron; Reinsch, Brian C; Tsyusko, Olga V; Bertsch, Paul M; Lowry, Greg V; Unrine, Jason M. Role of Particle Size and Soil Type in Toxicity of Silver Nanoparticles to Earthworms. *Soil Sci. Soc. Am. J 75* (2), 365–377.
23. Iavicoli, I; Fontana, L; Leso, V; Calabrese, E.J. Hormetic Dose Responses in Nanotechnology Studies. *Sci. Total Environ.* **2014**, *487*, 361–374.
24. Calabrese, E.J; Baldwin, L.A. Hormesis: U-Shaped Dose Responses and Their Centrality in Toxicology. *Trends Pharmacol. Sci* **2001**, *22* (6), 285–291.
25. Ma, Chuanxin; Chhikara, Sudesh; Minocha, Rakesh; Long, Stephanie; Musante, Craig; White, Jason C; Xing, Baoshan; Dhankher, Om Parkash. Reduced Silver Nanoparticle Phytotoxicity in Crambe Abyssinica with Enhanced Gluathione Production by Overexpressing Bacterial Gamma-Glutamylcysteine Synthase. *Environ. Sci. Technol* **2015**, *49* (16), 10117–10126.
26. Yin, Liyan; Cheng, Yingwen; Espinasse, Benjamin; Colman, Benjamin P; Auffan, Melanie; Wiesner, Mark; Rose, Jerome; Bernhardt, Emily S. More than the Ions: The Effects of Silver Nanoparticles on Lolium Multiflorum. *Environ. Sci. Technol* **2011**, *45* (6), 2360–2367.
27. Buzea, Cristina; Pacheco, Ivan I; Robbie, Kevin. Nanomaterials and Nanoparticles: Sources and Toxicity. *Biointerphases* **2007**, *2* (4), MR17–MR71.
28. Boxall, A; Chaudhry, Q; Sinclair, C; Jones, A; Aitken, R; Jefferson, B; Watts, C. Current and Future Predicted Environmental Exposure to Engineered Nanoparticles. *Central Science Laboratory* **2007**.

29. Siekkinen, Andrew R; McLellan, Joseph M; Chen, Jingyi; Xia, Younan. Rapid Synthesis of Small Silver Nanocubes by Mediating Polyol Reduction with a Trace Amount of Sodium Sulfide or Sodium Hydrosulfide. *Chemical Physics Letters* **2006**, *432*, 491–496.
30. Geitner, Nicholas K; Marinakos, Stella M; Guo, Charles; O'Brien, Niall; Wiesner, Mark R. Nanoparticle Surface Affinity as a Predictor of Trophic Transfer. *Environ. Sci. Technol* **2016**, *50* (13), 6663–6669.
31. Lee, Woo-Mi; Kwak, Jin Il; An, Youn-Joo. Effect of Silver Nanoparticles in Crop Plants Phaseolus Radiatus and Sorghum Bicolor: Media Effect on Phytotoxicity. *Chemosphere* **2012**, *86* (5), 491–499.
32. Nair, Remya; Varghese, Saino Hanna; Nair, Baiju G; Maekawa, T; Yoshida, Y; Kumar, D. Sakthi. Nanoparticulate Material Delivery to Plants. *Plant Science* **2010**, *179* (3), 154–163.
33. Kettler, K; Veltman, K; van de Meent, D; van Wezel, A; Hendriks, A.J. Cellular Uptake of Nanoparticles as Determined by Particle Properties, Experimental Conditions, and Cell Type. *Environ Toxicol Chem* **2014**, *33* (3), 481–492.
34. Mao, Aiqin; Jin, Xia; Gu, Xiaolong; Wei, Xiaoqing; Yang, Guoing. Rapid, Green Synthesis and Surface-Enhanced Raman Scattering Effect of Single-Crystal Silver Nanocubes. *J. Mol. Struct.* **2012**, *1021*, 158–161.
35. Halvorson, Rebecca A; Vikesland, Peter J. Surface-Enhanced Raman Spectroscopy (SERS) for Environmental Analyses. *Environ. Sci. Technol* **2010**, *44* (20), 7749–7755.
36. Lubick, Naomi. Nanosilver Toxicity: Ions, Nanoparticles-or Both? *Environ. Sci. Technol* **2008**, *42* (23), 8617.
37. Lowry, Gregory V; Hotze, E.M; Bernhardt, Emily S; Dionysiou, D.D; Pedersen, J.A; Wiesner, M.R; Xing, B. Environmental Occurrences, Behavior, Fate, and Ecological Effects of Nanomaterials: An Introduction to the Special Series. *J. Environ. Qual* **2010**, *39* (6), 1867–1874.
38. Lowry, Gregory V; Espinasse, Benjamin; Badireddy, Appala Raju; Richardson, Curtis J.; Reinsch, Brian C; Bryant, Lee D; Bone, Audrey J; Deonarine, Amrika; Chae, Soryong; Therezien, Mathieu; et al. Long-Term Transformation and Fate of Manufactured Ag Nanoparticles in a Simulated Large Scale Freshwater Emergent Wetland. *Environ. Sci. Technol 46* (13), 7027–7036.
39. Dimpka, Christian O; McLean, Joan E; Martineau, Nicole; Britt, David W; Haverkamp, Richard; Anderson, Anne J. Silver Nanoparticles Disrupt Wheat (Triticum Aestivum L.) Growth in a Sand Matrix. *Environ. Sci. Technol* **2013**, *47* (2), 1082–1090.
40. El-Temsah, Yehia Sayed; Joner, Erik J. Impact of Fe and Ag Nanoparticles on Seed Germination and Differences in Bioavailability during Exposure in Aqueous Suspension and Soil. *Environmental Toxicology* **2011**, *27* (1), 42–49.
41. Miralles, Pola; Church, Tamara L; Harris, Andrew T. Toxicity, Uptake, and Translocation of Engineered Nanomaterials in Vascular Plants. *Environ. Sci. Technol* **2012**, *46* (14), 9224–9239.

Appendices

Appendix A-AgNM Characterization and Analysis of Dose-Dependent AgNP Toxicity on *Lolium multiflorum, Solanum lycopersicum,* and *Lactuca sativa*

1. Methods

I. Long Term Soil Procedure

Synthetic soil was made for this experiment following the Organisation for Economic Co-operation and Development (OECD) guidelines: 70% quarts silica sand (Quikrete, Atlanta, GA, USA), 20% EPK Kaolin clay (Edgar Minerals, Hawthorne, FL, U.S.A.), and 10% sphagnum peat moss (Scott's Miracle-Gro Co., Marysville, OH, USA) .[18,19] Four hundred grams of homogenous soil was added to each 4"x4" pot, with 9 seeds of either *Lolium multiflorum, Solanum lycopersicum,* or *Lactuca sativa*, as shown in Figure 4. An initial 50 mL dose of PicoPure water and AgNP solutions at doses of 1 ppm, 5 ppm, 10 ppm, 50 ppm, or 100 ppm were added to each pot. For the following 29 days, each pot was watered daily with between 10 mL and 30 mL of PicoPure water to maintain saturated soil. Temperature and humidity were monitored three times per day to ensure a consistent growth environment. After 27 d, roots and shoots were extracted from soil, separated from one another, and length was measured individually.

II. Analysis of Phytotoxicity

Root and shoot length for the unique AgNM shapes and doses were measured using digital calipers to discover potential differences. Statistical analysis of the root and shoot length of the long-term study was carried out using 2-way factorial Analysis of Variance (ANOVA) in JMP 13 Pro Software (SAS Institute Inc., Cary, NC, U.S.A). Tukey-Kramer analysis was conducted to determine differences between doses of AgNPs in *L. multiflorum, S. lycopersicum* and *L. sativa* roots and shoots. Statistically significant differences in Tukey-Kramer analysis, where $p<0.05$,

were indicated with a letter change: A, B, C. A combination of letters, such as AB, indicated differences significant at $p<0.1$. Values are plotted as mean ± standard error.

2. Results

I. AgNM Characterization

Figure A1 shows the AA spectroscopy calibration curve to determine concentrations of Ag in the solutions. These values were later utilized to prepare various doses of AgNMs for the soil study. The calibration curve points showed a regression R^2 value of 0.99729.

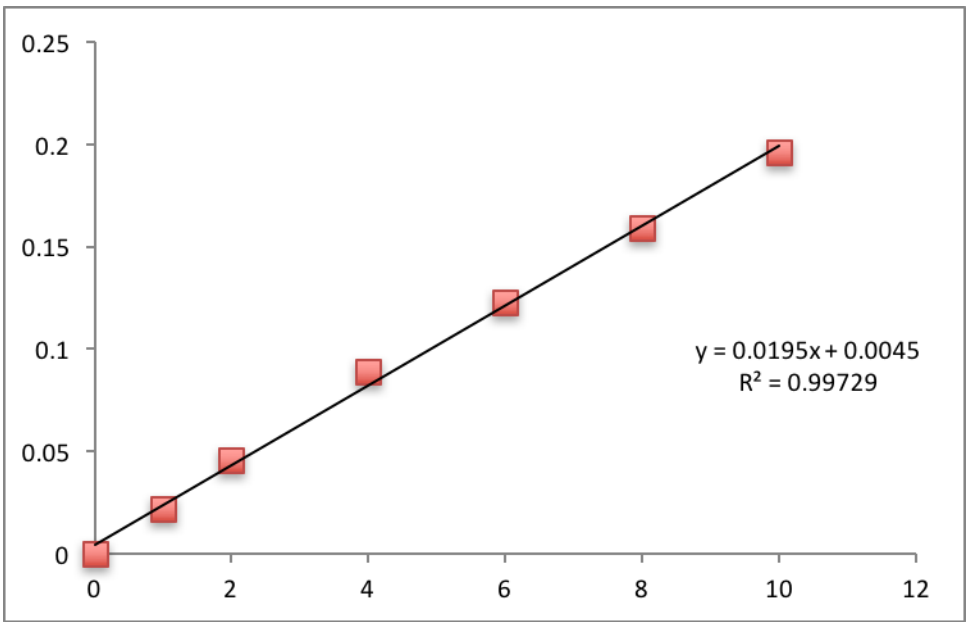

Figure A1. Atomic absorption concentration calibration curve for AgNMs (ppm).

II. AgNM on *L. multiflorum* growth

Figures A2, A3, A4, and Table A1 show the analysis of shape-dependent toxicity of AgNPs, AgNCs, and AgNWs on the roots and shoots of *L. multiflorum*. This data compared the mean root and shoot lengths of the plants, and their respective standard errors, of the control condition and doses of 1 ppm, 5 ppm, 10 ppm, 50 ppm, and 100 ppm Ag. Tukey-Kramer

analysis was conducted in JMP 13 Pro Software to compare significant differences in root and shoot length within the dose range, with 0 ppm indicating the control.

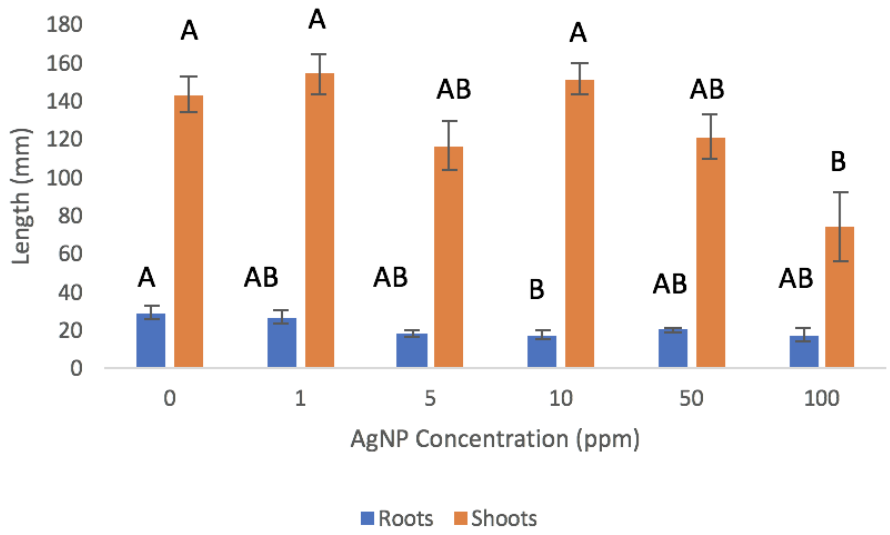

Figure A2. Dose-dependent growth of AgNPs on *L. multiflorum* roots and shoots. Different letters represent significant differences at $p<0.05$.

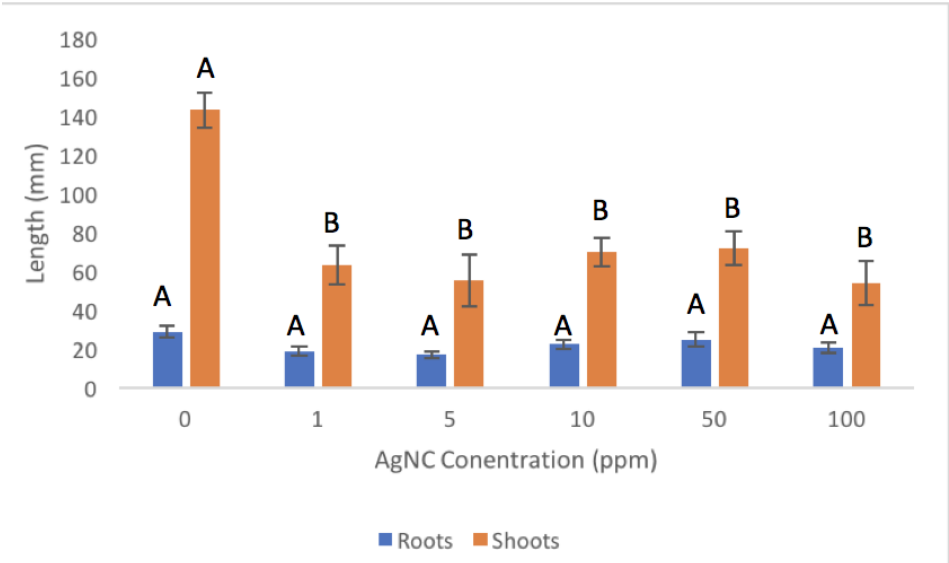

Figure A3. Dose-dependent growth of AgNCs on *L. multiflorum* roots and shoots. Different letters represent significant differences at $p<0.05$.

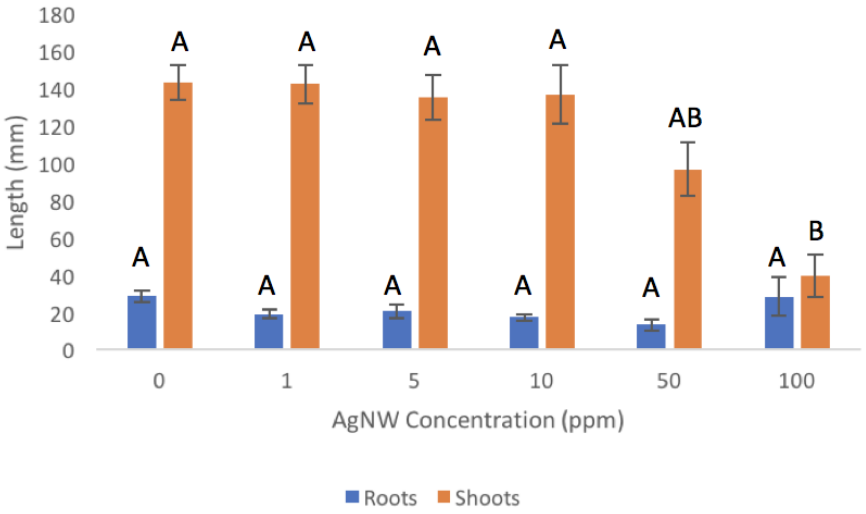

Figure A4. Dose-dependent growth of AgNWs on *L. multiflorum* roots and shoots. Different letters represent significant differences at $p<0.05$.

Table A1. Shape-dependent toxicity with mean and standard error root and shoot lengths of *L. multiflorum* (in mm). Significant differences in lengths are indicated by letters from Tukey-Kramer Analysis.

Species	**Roots**			**Shoots**		
AgNPs	Concentration (ppm)		Mean	Concentration (ppm)		Mean
	0	A	28.77 ± 3.2	1	A	153.84 ± 10.3
	1	A B	26.26 ± 3.5	10	A	151.36 ± 8.1
	50	A B	19.80 ± 1.5	0	A	143.25 ± 9.2
	5	A B	17.77 ± 2.0	50	A B	121.06 ± 11.4
	100	A B	16.95 ± 3.6	5	A B	116.22 ± 12.8
	10	B	16.30 ± 2.6	100	B	73.67 ± 18.0
AgNCs	Concentration (ppm)		Mean	Concentration (ppm)		Mean
	0	A	28.77 ± 3.2	0	A	143.25 ± 9.2
	50	A	24.68 ± 3.6	50	B	72.09 ± 8.6
	10	A	22.39 ± 2.4	10	B	69.69 ± 7.4
	100	A	20.47 ± 2.6	1	B	63.43 ± 10.0
	1	A	18.77 ± 2.4	5	B	55.35 ± 13.5
	5	A	16.95 ± 1.6	100	B	53.60 ± 11.4
AgNWs	Concentration (ppm)		Mean	Concentration (ppm)		Mean
	0	A	28.77 ± 3.2	0	A	143.25 ± 9.2
	100	A	28.57 ± 10.3	1	A	142.50 ± 10.2
	5	A	20.70 ± 3.8	10	A	136.96 ± 15.5
	1	A	19.31 ± 2.4	5	A	135.24 ± 12.1
	10	A	17.52 ± 1.7	50	A B	96.75 ± 14.4
	50	A	13.44 ± 3.2	100	B	39.78 ± 11.1

During analysis of shape-dependent solutions of *L. multiflorum* (Figures A2, A3, A4) and the mean lengths (Table A1), there also appears to be shape-dependent inconsistencies between doses. AgNP exposed roots and shoots indicated some significant decrease in mean length at 10 ppm in roots and 100 ppm in shoots, as well as decreased length at all doses compared to the control. AgNCs had decreased root length at all values compared to the control, but these differences were not significant. The shoots exposed to AgNCs, however, showed significant decreases in length at all doses compared to the control. All root doses of

AgNWs showed non-significant decreased lengths compared to the control. The shoots showed more significant toxicity than its roots: all doses had less growth compared to the control, but the only significant decrease in length was at the 100 ppm dose. Within *L. multiflorum* shoots, all shapes showed significant dose-dependence, while the roots showed insignificant dose-dependence, compared to the control.

III. AgNP Toxicity in Different Plant Species

Figures A2, A5, A6, and Table A2 indicated the analysis of dose-dependent toxicity of AgNPs on the roots and shoots of all three plant species. This data compared the mean root and shoot lengths of the plants, and their respective standard errors, of the control condition and doses of 1 ppm, 5 ppm, 10 ppm, 50 ppm, and 100 ppm. Tukey-Kramer analysis was conducted in JMP 13 Pro Software (SAS Institute Inc., Cary, NC, U.S.A.) to compare significant differences in root and shoot mean length within the concentration range, with 0 ppm indicating the control.

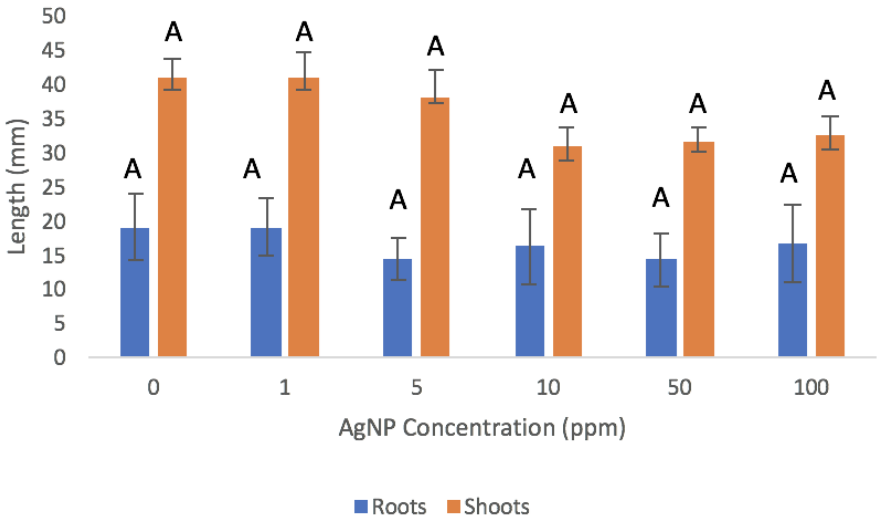

Figure A5. Dose-dependent growth of AgNPs on *S. lycopersicum* roots and shoots. Different letters represent significant differences at $p<0.05$.

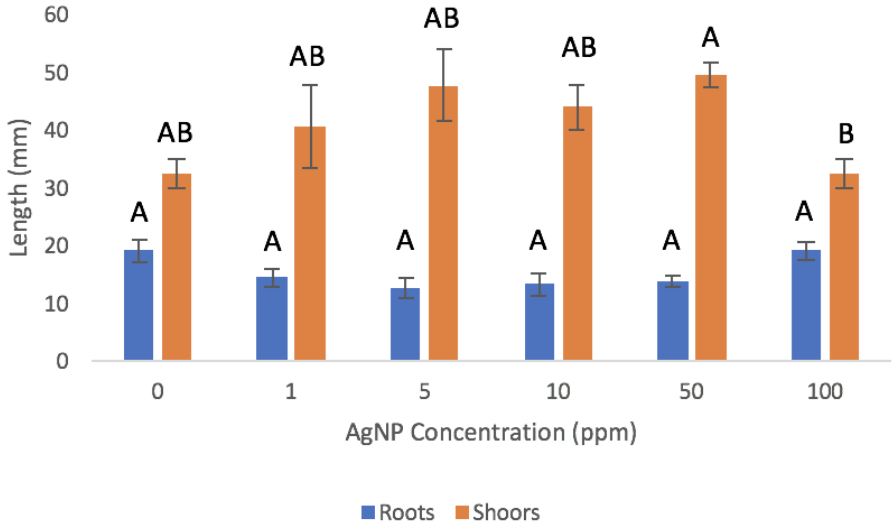

Figure A6. Dose-dependent growth of AgNPs on *L. sativa* roots and shoots. Different letters represent significant differences at $p<0.05$.

Table A2. Dose-dependent toxicity with mean and standard error root and shoot lengths of AgNPs on *L. multiflorum*, *S. lycopersicum*, and *L. sativa* (in mm). Significant differences in lengths are indicated by letters from Tukey-Kramer Analysis.

Species	**Roots**			**Shoots**		
L. multiflorum	Concentration (ppm)		Mean	Concentration (ppm)		Mean
	0	A	28.77 ± 3.2	1	A	153.84 ± 10.3
	1	A B	26.26 ± 3.5	10	A	151.36 ± 8.1
	50	A B	19.80 ± 1.5	0	A	143.25 ± 9.2
	5	A B	17.77 ± 2.0	50	A B	121.06 ± 11.4
	100	A B	16.95 ± 3.6	5	A B	116.22 ± 12.8
	10	B	16.30 ± 2.6	100	B	73.67 ± 18.0
S. lycopersicum	Concentration (ppm)		Mean	Concentration (ppm)		Mean
	0	A	19.07 ± 1.7	0	A	40.95 ± 2.7
	1	A	18.96 ± 1.6	1	A	40.86 ± 3.8
	100	A	16.60 ± 2.1	5	A	38.17 ± 3.8
	10	A	16.22 ± 2.1	100	A	32.55 ± 2.8
	5	A	14.27 ± 1.0	50	A	31.55 ± 2.0
	50	A	14.27 ± 1.4	10	A	30.77 ± 3.0
L. sativa	Concentration (ppm)		Mean	Concentration (ppm)		Mean
	100	A	19.06 ± 1.7	50	A	49.70 ± 2.1
	0	A	18.58 ± 2.3	5	A B	47.75 ± 6.1
	1	A	14.38 ± 1.6	10	A B	43.88 ± 3.9
	50	A	13.65 ± 1.0	1	A B	40.55 ± 7.3
	10	A	13.33 ± 1.9	0	A B	33.32 ± 2.9
	5	A	12.58 ± 1.8	100	B	32.31 ± 2.6

Upon examination of AgNP dose-dependent solutions with all three plants (Figures A2, A5, A6) and the mean lengths (Table A2), there appears to be dose-dependent toxicity inconsistencies between plant species. AgNM toxic effects and transport mechanisms have not shown to be universal between plant species, as well as between their roots and shoots, so multiple plants must be analyzed and compared.[26] *L. multiflorum* roots and shoots indicated significant decreases in mean length at 10 ppm in roots and 100 ppm in shoots ($p<0.05$), as well as decreased length at all doses compared to the control ($p<0.10$ for all roots and 50 ppm and

5 ppm in shoots). Both AgNP-dosed *S. lycopersicum* roots and shoots showed decreased length compared to the control, though it was not significant at any dose. In *L. sativa,* the roots exhibited no significant differences in growth, while the shoots showed an inconsistent trend in toxicity. Doses of 1 ppm, 5 ppm, 10 ppm, and 50 ppm showed an increase in growth ($p<0.1$), and the 100 ppm dose showed a decrease in growth compared to the control ($p<0.05$). This enhanced growth, known as the hormetic effect, has been observed in previous literature with AgNM toxicity studies.[27,28]

Appendix B-Safety Considerations

Numerical codes used to indicate the extend of the hazard are: 0=no known hazard, 1=slight, 2=moderate, 3=severe, and 4=extreme. Abbreviations used for personal protective equipment (PPE) are: **G**=goggles, **G&S**=goggles and face shield, **LC**=lab coat, **LC&A**=lab coat and apron, and **H**=vented hood. Abbreviations used for types of gloves include: **R**=rubber, **PVC**=polyvinyl chloride, **BV**=butyl viton, **Nit**=nitrile, **Neo**=neoprene. For Standard Operating Procedures (SOPs), "RD" indicates that it was provided by the research director. Citations given for other sources of SOP are formatted as (author, year).

Table 1. Summary of chemical hazards and mitigations.

Chemical	CAS RN	Health	Fire	Reactivity	Contact	PPE	SOP
Ethylene glycol	107-21-1	1	1	0	Acute oral toxicity, skin irritant, eye irritant	G, Nit gloves, LC	RD
Iron nitrate nonahydrate	7782-61-8	2	0	1	Oxidizer, harmful if inhaled or swallowed, eye irritant, skin	G, Nit gloves, LC	RD

					irritant, respiratory tract infection		
Nitric acid	7697-37-2	3	0	0	Oxidizer, severe burn to skin, lung damage	G, Nit gloves, LC	RD
PVP	9003-39-8	1	1	0	Oral toxicity, chronic health effectss	G, Nit gloves, LC	RD
Silver nitrate	7761-88-8	3	1	3	Corrosive	G, Nit gloves, LC	RD
Sodium chloride	7647-14-5	1	1	0	Skin irritant, eye irritant, hazardous to ingest and inhale	G, Nit gloves, LC	RD
Sodium hydroxide	1310-73-2	3	0	1	Corrosive, skin burns	G, Nit gloves, LC	RD
Sodium sulfide nonahydrate	1313-84-4	3	1	1	Skin burns	G, Nit gloves, LC	RD

Table 2. Summary of physical hazards and mitigations

Equipment	**Hazard**	**PPE**	**SOP**
Hot plate	Burning	G, LC, Nit gloves	RD
Syringe Needles	Toxic materials could enter bloodstream	G, LC, Nit Gloves	RD

Table 3. Summary of biological hazards and mitigations.

Equipment	**Hazard**	**PPE**	**SOP**
None	None	None	None

Appendix C-Table of Terms and Acronyms used in Research Project

Term/Acronym/Abbreviation	Explanation
AA	**Atomic absorption spectroscopy:** An analytical tool using absorption to determine concentration of NM solutions.
AgNCs	**Silver Nanocubes:** Structures that are monodisperse, non-aggregated silver cube structures averaging 38 nanometers.
AgNMs	**Silver Nanomaterials:** The three silver nanostructures discussed in this proposal, including silver nanoparticles, silver nanocubes, and silver nanowires.
AgNPs	**Silver Nanoparticles:** Structures that are monodisperse, non-aggregated spherical particles with antimicrobial properties, averaging approximately 41 nanometers.
AgNWs	**Silver Nanowires:** Structures that are monodisperse, non-aggregated wires averaging a length of 4650 nanometers, and averaging a width of 78 nanometers.
ANOVA	**Analysis of Variance:** A method of statistical analysis used to analyze the differences among group means.
L. multiflorum	***Lolium multiflorum:*** Ryegrass native to temperate Europe, used as a cover crop in agriculture to prevent erosion.
L. sativa	***Lactuca Sativa:*** Lettuce.
nm	**Nanometers:** The unit (10^{-9} meters) used with TEM and SEM1 to measure length and width of the various synthesized AgNMs.
OECD	**Organisation for Economic Co-operation and Develpment**
ppm	**Parts per million:** A unit of measuring concentration
PVP	**Polyvinylpyrrolidone:** A water-soluble polymer that coats the silver nanomaterials to minimize dissolution into the aqueous environment
SEM	**Scanning electron microscope:** Used to characterize and measure the size of AgNMs.
S. lycopersicum	***Solanum lycopersicum:*** tomato

TEM	**Transmission electron microscopy:** Used to characterize and measure the size of AgNMs.
UV-Vis	**Ultraviolet-vsible spectroscopy:** used to characterize AgNMs with absorption peaks at specific wavelengths.